

Supporting Information

Carbon within carbon: Growth of excitation-independent CDs within functional mesoporous carbon towards detection and adsorption of specific nitrofurans class of antibiotics†

Sanjay Yadav,^{*ab} Nishu Choudhary,^{ab} and Alok Ranjan Paital^{*ab}

^a*Salt and Marine Chemicals Division, CSIR-Central Salt & Marine Chemicals Research Institute, G.B. Marg, Bhavnagar-364002, Gujarat, India. E-mail: arpaital@csmcri.res.in; sychem00700@gmail.com*

^b*Academy of Scientific and Innovative Research (AcSIR), Ghaziabad-201002, India.*

Sr. No	Contents	Page No.
1	Materials & Instrumentation	S2-3
2	The synthetic mechanism of the final material, EDX Elemental mapping & analysis (Fig. S1-S3)	S3-4
3	Pore size parameters & Raman spectra (Fig. S4 & S5)	S4-5
4	The full scan XPS spectra of the synthesized Ordered mesoporous carbon (OMC) (Fig. S6) and the core level Si-2p & O 1s XPS spectra of the aminated OMC (OMC@NH ₂) (Fig. S7).	S5-6
5	The core level Si-2p XPS spectra of the final material CD@OMC@NH ₂ , & UV-Vis analysis (Fig. S8 & S9)	S6-7
6	The excitation independent parameters & relative fluorescence quenching efficiency (Fig. S10 & S11)	S7-8
7	The TCSPC results (Table S1) & LOD, L-R plots (Fig. S12 & S13)	S8-9
8	The RET mechanism spectral plot, IFE corrected fluorescence quenching efficiency plots (Fig. S14 & S15) the calibration plots of the NFT & FZD antibiotic	S9-11
9	The characterization of the regenerated material (FTIR comparison, fluorescence blank reading and FeSEM image (Fig. S16).	S12

Materials: All the chemicals and reagents employed in chemical processing and synthetic procedures were of analytical grade. The chemical synthesis involved the use of dry solvents, which were utilized as they were without any additional purification steps. [Bmim]Cl, Pluronic F127, Iminodiacetic acid (IDA), orthophenylenediamine, 3-Aminopropyltriethoxysilane (3-APTES) and all antibiotics were purchased from Merck (Sigma-Aldrich) & TCI chemical private Ltd. Dry toluene, Milli Q water, HCl, NaOH, methanol, chloroform, ethanol & were purchased from Spectrochem Pvt. Ltd.

Instrumentation: The Shimadzu UV 3101PC spectrophotometer and Edinburg Instruments model Xe-900 were employed to capture absorption and fluorescence emission spectra, using a 350 nm excitation source, in an aqueous dispersion medium. For structural characterization, FTIR spectra were measured using a Perkin-Elmer GX spectrophotometer (manufactured in the USA) with KBr pellets. Surface area measurements were conducted using the micromeritics 3 FLEX instrument, with the sample being activated at 55 °C for 45 min before analysis. To determine surface morphology, scanning electron microscopy (SEM-Leo series 1420 VP) equipped with INCA and transmission electron microscopy (TEM) using a JEOL JEM 2100 microscope was employed, both using Lacey carbon-coated grids. X-ray photoelectron spectroscopy (XPS) was used for chemical and surface state analysis, with a Thermo Fisher Nexsa spectrophotometer recording the spectra using monochromated Al K α radiation with an energy of 1486.6 eV. The ICP-MS Thermofisher icap Qnova series instrument was utilized for metal ion concentration determination, with samples being filtered using Thermo Fisher syringe filters (0.45 μ m). Powder X-ray diffraction profiles were recorded using a MiniFlex-II (FD 41521) powder diffractometer from Rigaku, Japan, with a scan rate of 1° per degree. Fluorescence lifetime measurements were performed using TSPC experiments on an Edinburg

instrument OB 920 fluorescence spectrophotometer equipped with a pulse diode laser (Laser-EPLED-350 nm) as the excitation source.

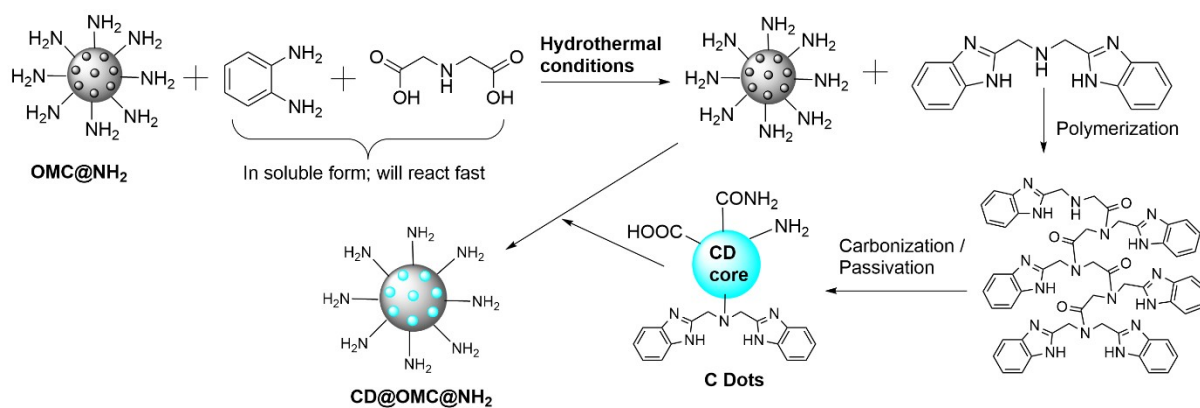


Fig. S1 The mechanistic representation of the synthesis of the final material CD@OMC@NH₂.

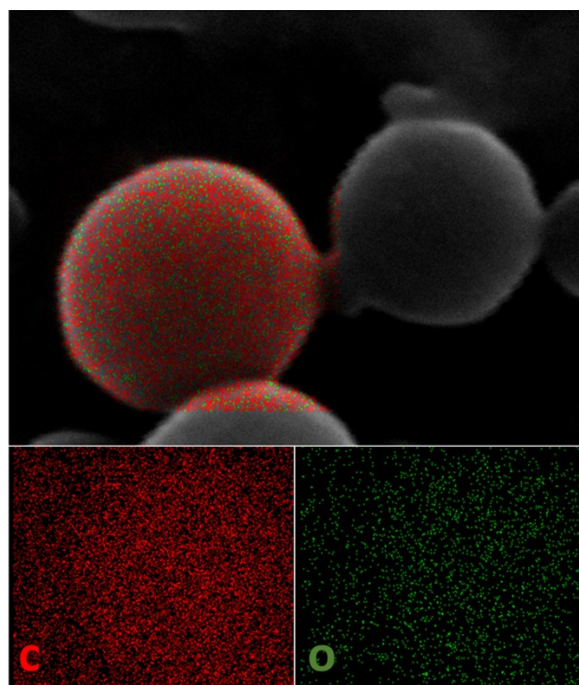


Fig. S2 The FeSEM elemental mapping of the synthesized ordered mesoporous carbon spheres (OMC) showing carbonaceous nature.

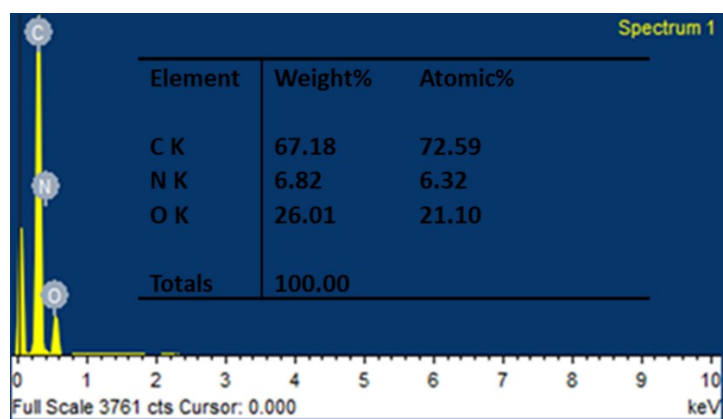


Fig. S3 The Energy dispersive X-ray (EDX) spectra of the synthesized ordered mesoporous carbon (OMC) (inset: chemical composition table).

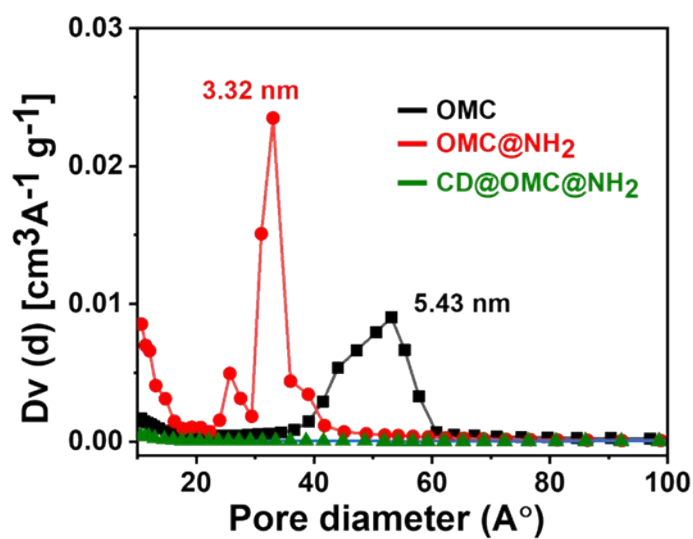


Fig. S4 The pore size parameters of the synthesized materials.

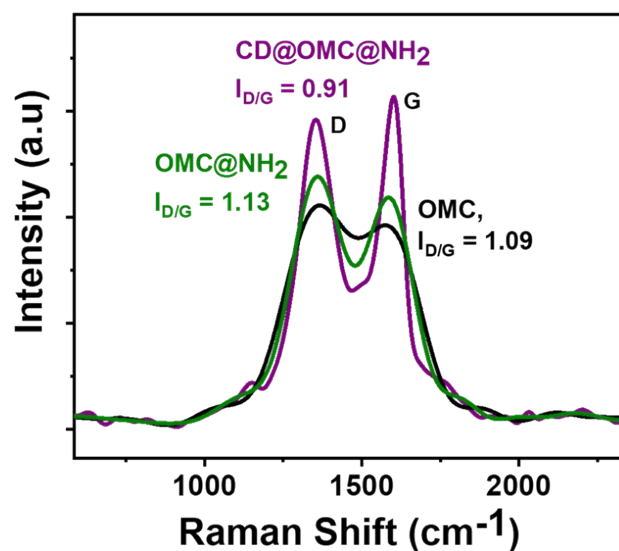


Fig. S5 The comparison of the Raman spectra profiles of the synthesized ordered mesoporous carbon (OMC), OMC@NH₂ and CD@OMC@NH₂ materials.

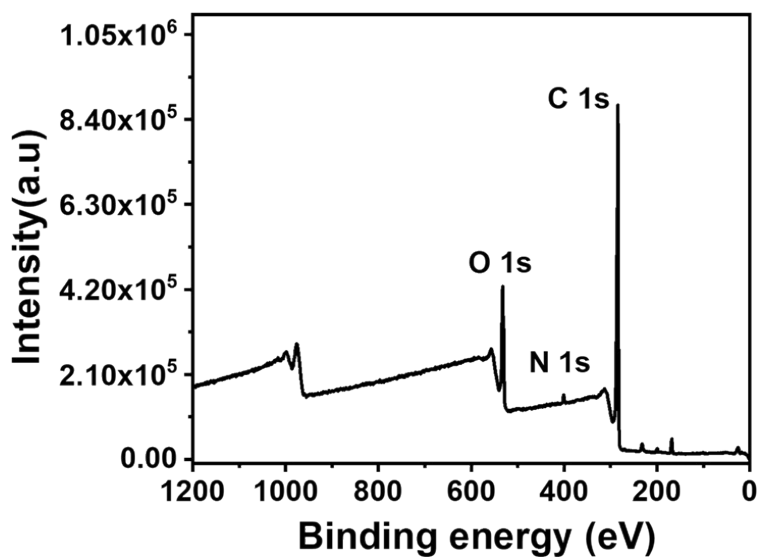


Fig. S6 The full scan XPS spectra of the synthesized Ordered mesoporous carbon (OMC).

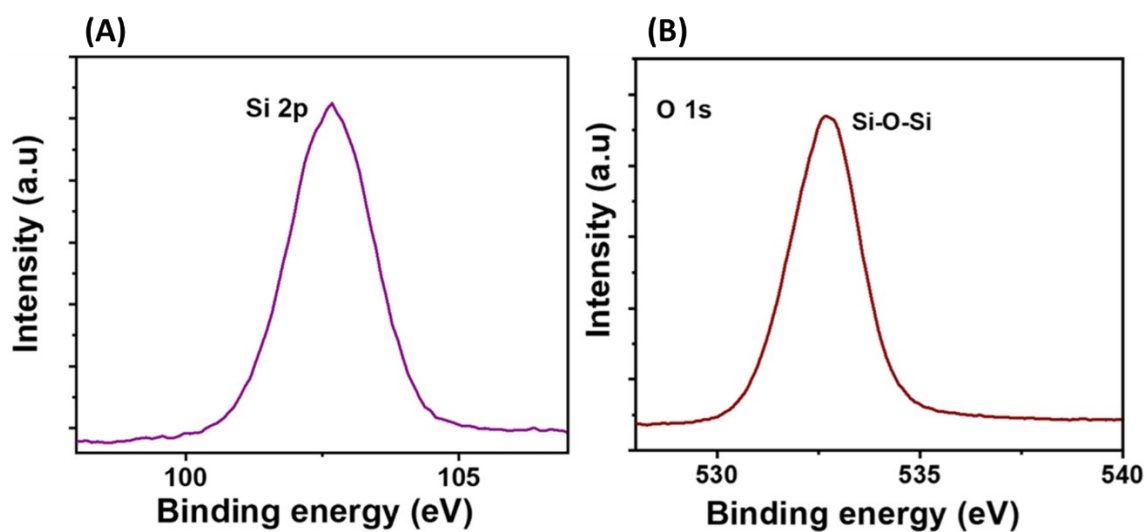


Fig. S7 The core level Si-2p & O 1s XPS spectra of the aminated OMC (OMC@NH₂).

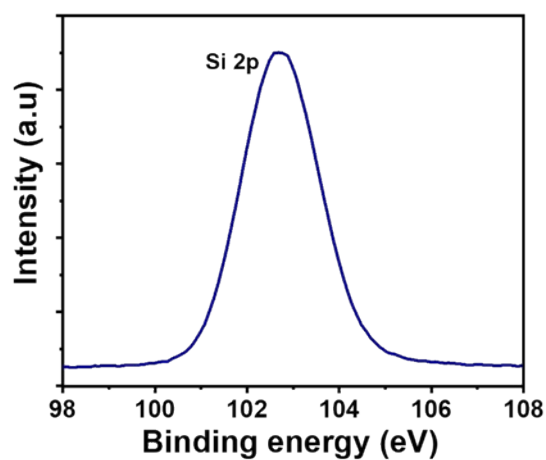


Fig. S8 The core level Si-2p XPS spectra of the final material CD@OMC@NH₂.

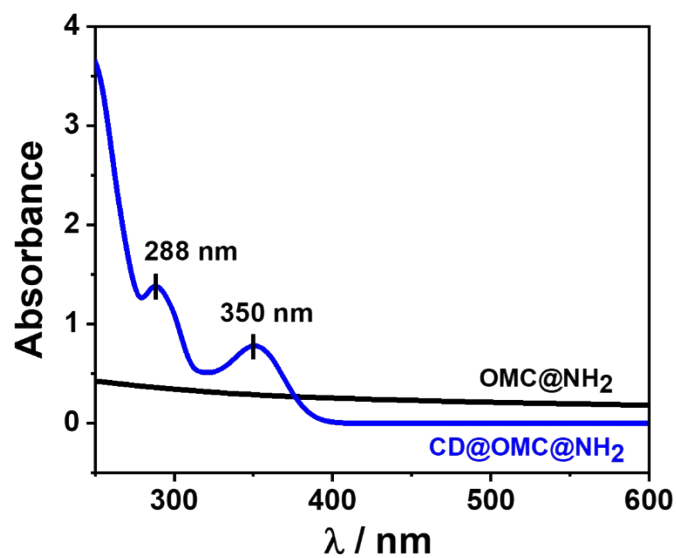


Fig. S9 The UV-Vis profile of the OMC & carbon dot encapsulated final material CD@OMC@NH₂.

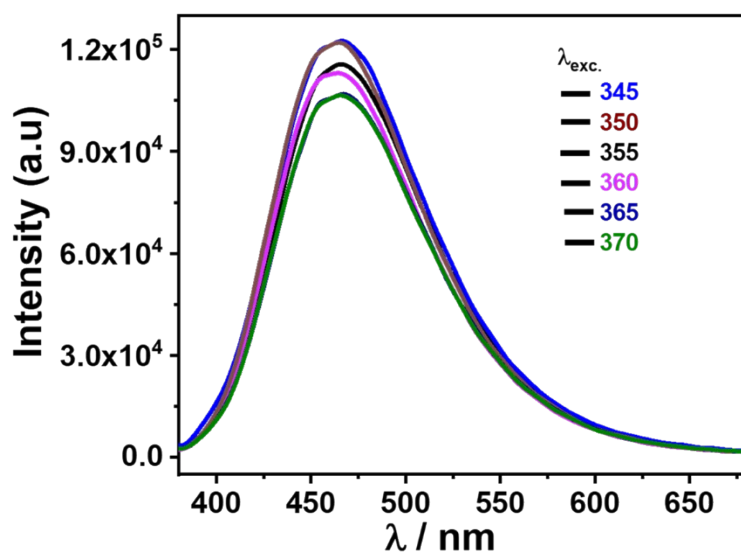


Fig. S10 The fluorescence emission intensity plot of the final material CD@OMC@NH₂ at various excitation wavelengths (345-370 nm) showing excitation-independency.

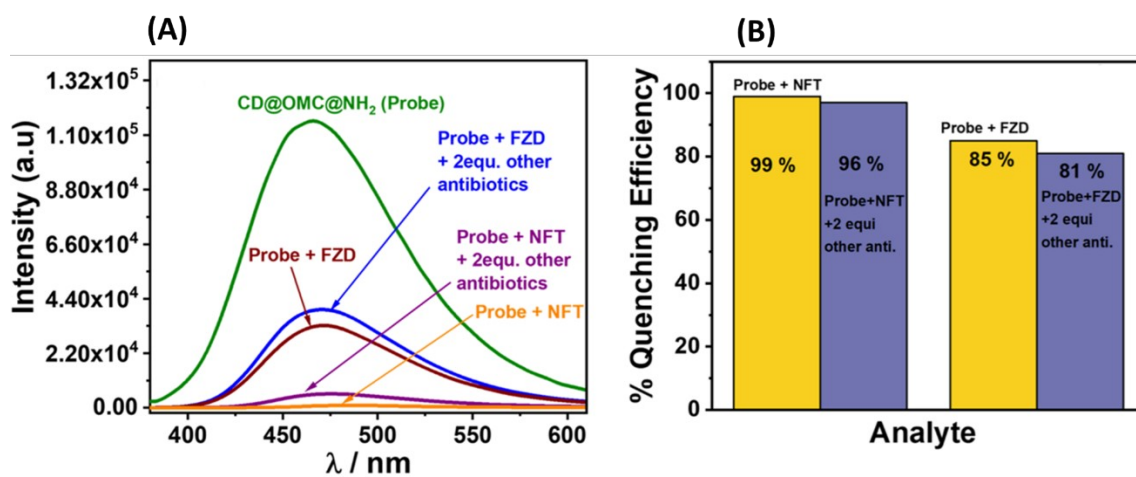


Fig. S11 The fluorescence interference study & the relative quenching efficiency in the presence of 2 equivalents of other antibiotics (except the interfering antibiotics).

Table S1. The fluorescence lifetime measurements of the final probe materials (CD@OMC@NH₂)

Sample	τ (ns)	Percentage (%)	χ^2
CD@OMC@NH ₂ (Probe)	2.62	100	0.99
Probe + 2 μ M NFT	2.38	100	0.99
Probe + 4 μ M NFT	2.01	100	1.08
Probe + 6 μ M NFT	1.23	100	0.99
Probe + 1 μ M FZD	2.41	100	0.99
Probe + 2 μ M FZD	2.21	100	1.01
Probe + 3 μ M FZD	1.63	100	1.10

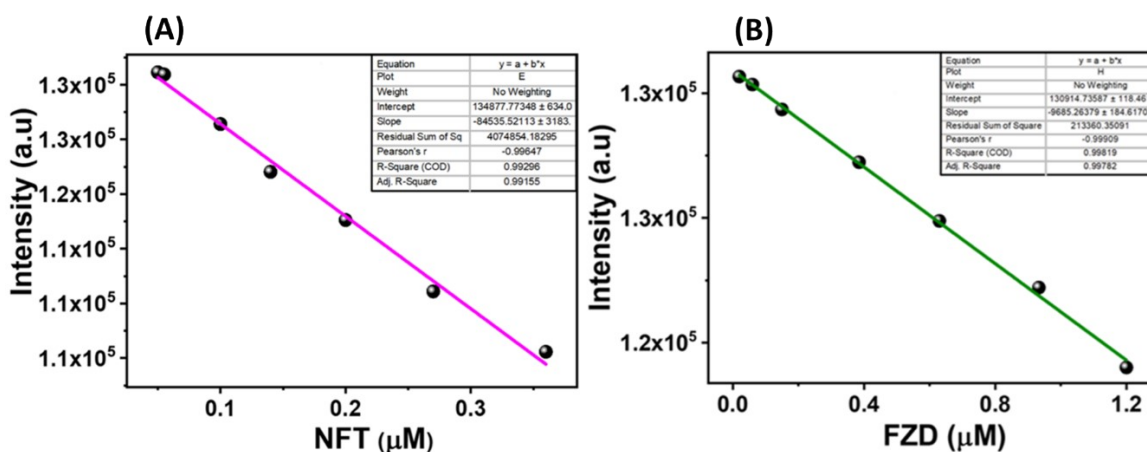


Fig. S12 The LOD Plots towards the specific antibiotics Nitrofurantoin (NFT) and Furazolidone (FZD).

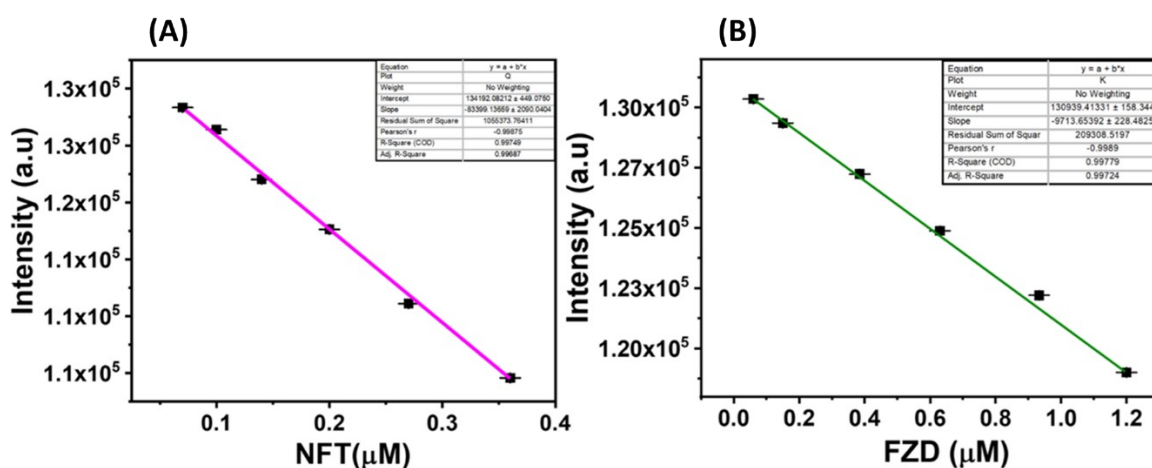


Fig. S13 The Linear range (L-R) Plots towards the specific antibiotics Nitrofurantoin (NFT) and Furazolidone (FZD).

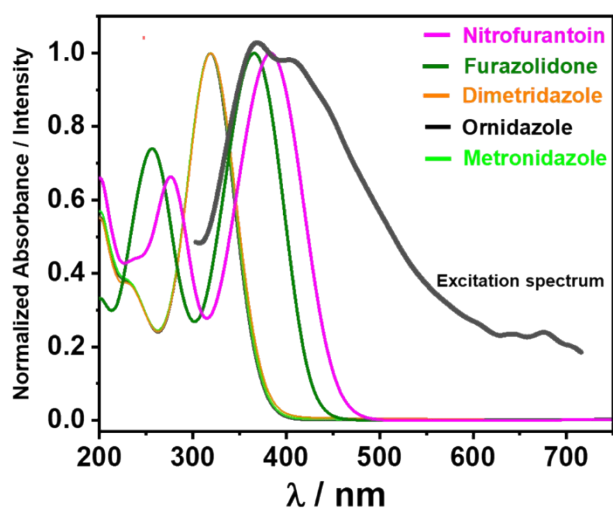


Fig. S14 The spectral overlap plot between the excitation spectrum of the final material and absorbance of the antibiotics showing inner filter effect (IFE).

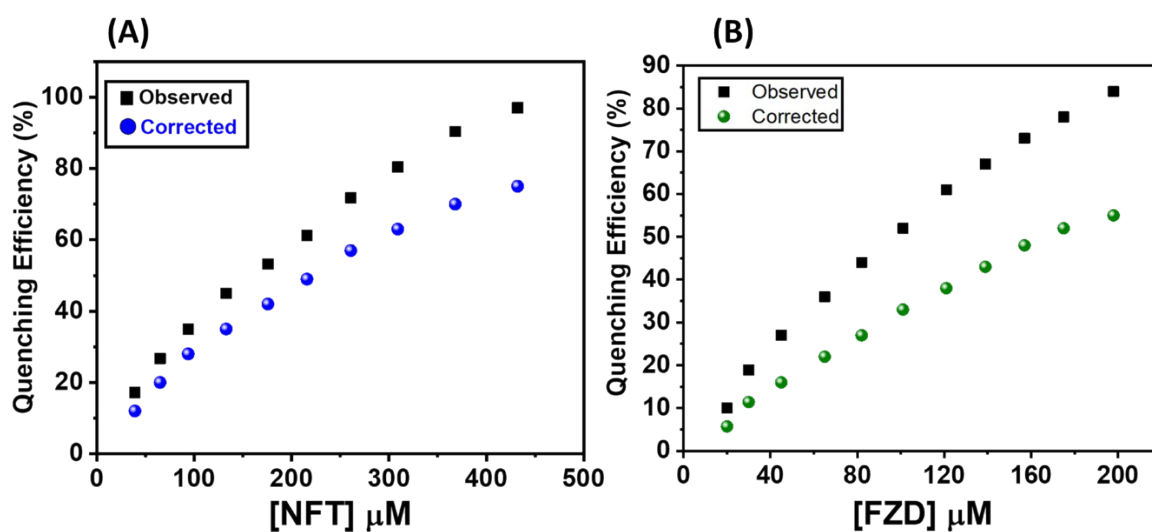


Fig. S15 The observed and corrected fluorescence quenching efficiency (%) of the probe material towards NFT and FZD antibiotics.

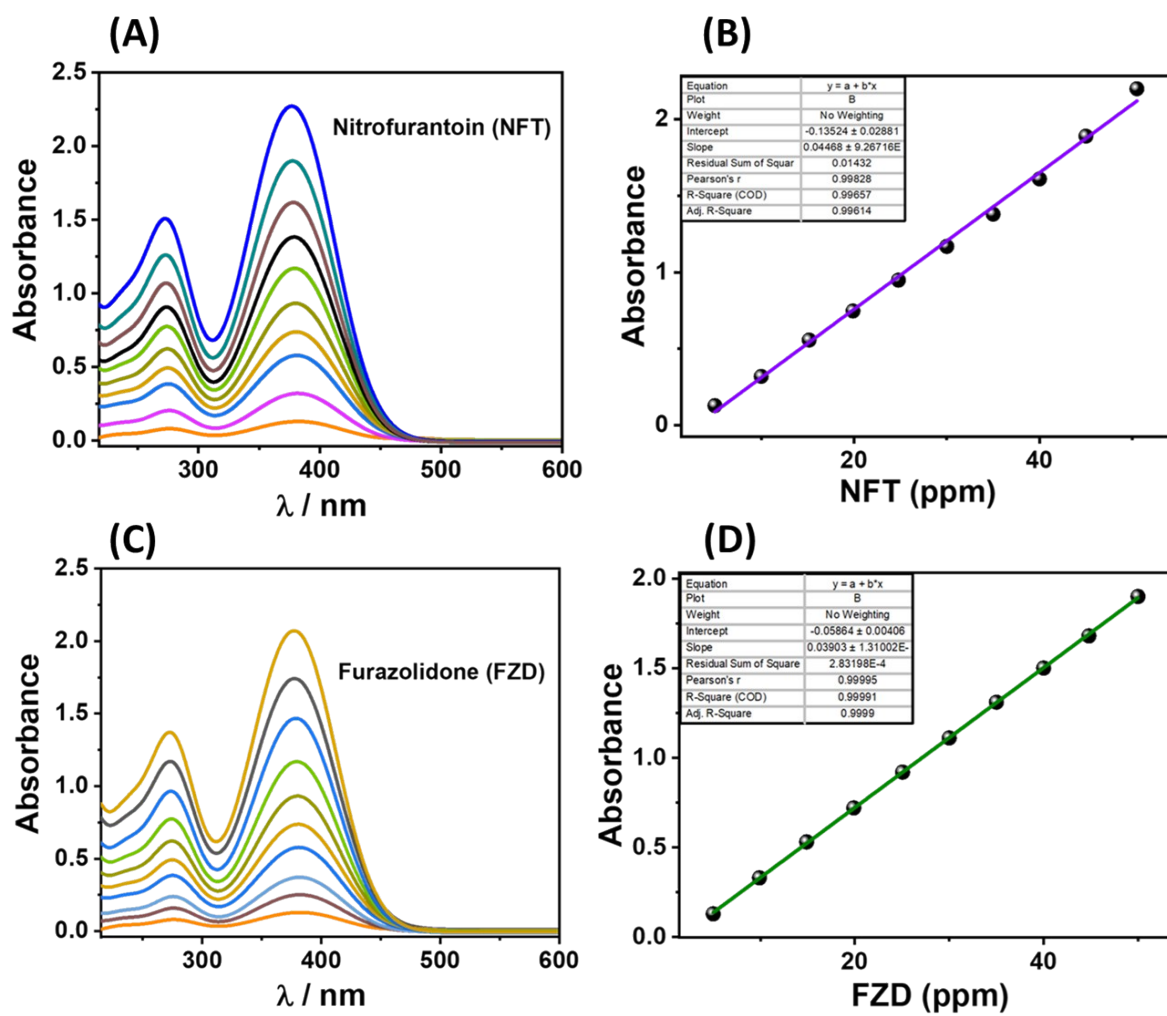


Fig. S16 The UV-Vis calibration spectra and the plot of absorbance vs. concentration of NFT & FZD antibiotic.

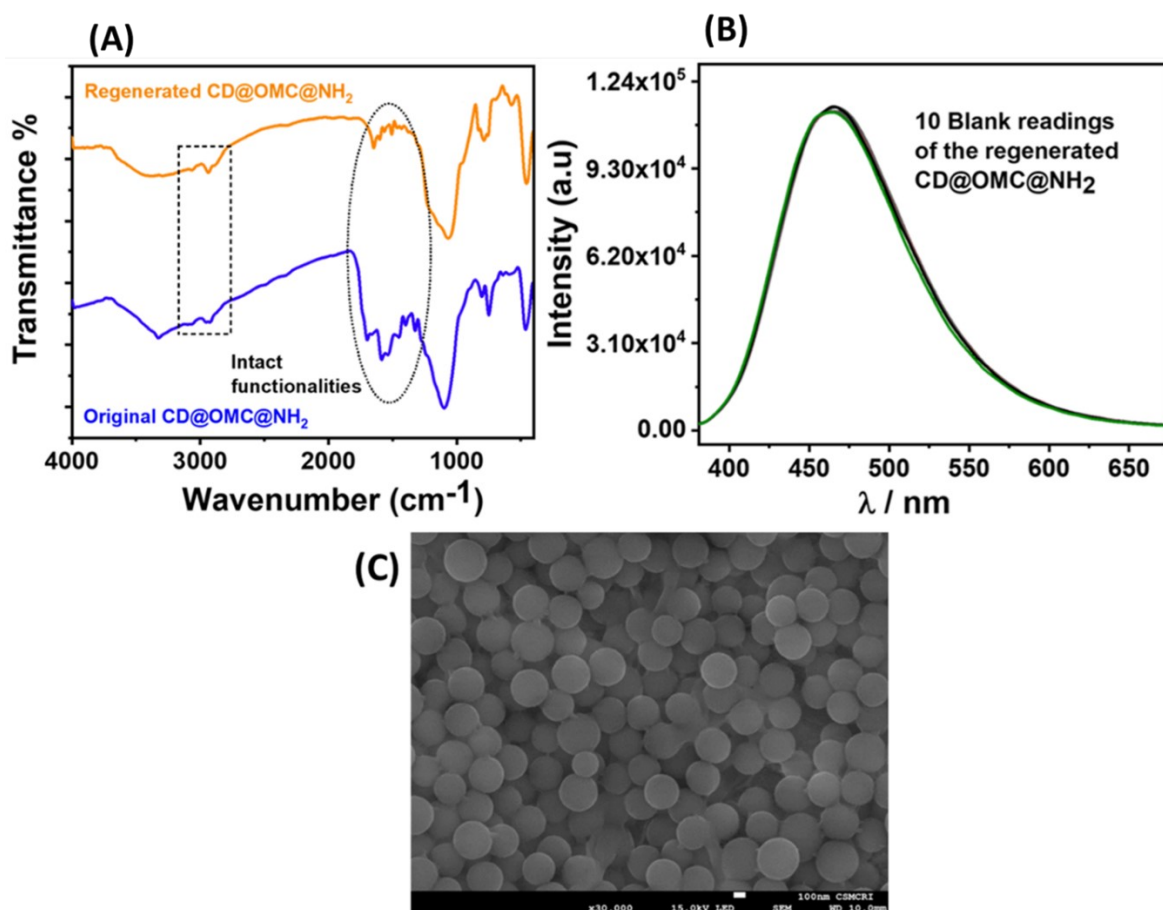


Fig. S17 (A) The comparison of the FT-IR spectra of the original and regenerated material CD@OMC@NH₂ exhibiting intact functionalities. (B) The blank fluorescence reading of the regenerated material shows a similar optical response to that of the original material. (C) The high-resolution SEM image of the regenerated material shows surface regularity.